

THESIS FOR THE DEGREE OF DOCTOR OF PHILOSOPHY

In

SOLID AND STRUCTURAL MECHANICS

Optimisation of Railway Switches and Crossings

BJÖRN A. PÅLSSON

Department of Applied Mechanics
CHALMERS UNIVERSITY OF TECHNOLOGY
Göteborg, Sweden 2014

Optimisation of Railway Switches and Crossings
BJÖRN A. PÅLSSON
ISBN 978-91-7385-978-3

© BJÖRN A. PÅLSSON, 2014

Doktorsavhandlingar vid Chalmers Tekniska Högskola
Ny serie nr 3659
ISSN 0346-718X

Department of Applied Mechanics
Chalmers University of Technology
SE-412 96 Göteborg
Sweden
+46 (0)31-772 1000

Cover: Railway crossing

Chalmers Reproservice
Göteborg, Sweden 2014

Optimisation of Railway Switches and Crossings
BJÖRN A. PÅLSSON
Department of Applied Mechanics
Chalmers University of Technology, SE-412 96, Göteborg, Sweden
E-mail: bjorn.palsson@chalmers.se

Abstract

Methods for simulation-based optimisation of the design of railway turnouts (switches & crossings, S&C) are developed and demonstrated. Building on knowledge of dynamic wheel–rail interaction in turnouts, it is investigated how rail profile degradation can be reduced by the optimisation of geometry and component stiffness of the track superstructure. It is assumed that reduced rail profile degradation will reduce the Life Cycle Cost (LCC) of turnouts.

In order to obtain robust optimised designs that perform well in situ, the influence of spread in traffic parameters, such as wheel profile and wheel–rail friction coefficient, is accounted for in the optimisations. For this purpose, studies of the correlation between wheel profile characteristics and damage in S&C are performed to allow for an efficient parameter sampling using the Latin Hypercube Sampling method.

Track gauge optimisation in the switch panel is performed using a multi-objective optimisation approach to highlight the design trade-off in performance between different traffic routes and moves. The objective is to minimise rail and wheel wear as estimated by the energy dissipation in the wheel–rail contacts. As track gauge widening affects the switch rail design, the switch rail geometry is linked to the gauge widening in the parameterisation. It is found that gauge configurations with a large maximum gauge widening for the straight stock rail are optimal for both the through and diverging routes, while the results for the curved stock rail show a more significant route dependence.

A method for the optimisation of switch rail profile geometry is presented, where the geometry parameterisation is inspired by a manufacturing process for switch rails. It is found that increased profile height and increased profile shoulder protuberance are preferred to reduce the energy dissipation and wheel–rail contact pressures when a nominal S1002 wheel profile is used as input. It is concluded that accurate constraints on allowable switch rail loading need to be established to determine the feasible design space for switch rail geometry optimisation.

A method for the optimisation of crossing geometry is also introduced. The rail cross-sections are optimised for minimum wheel–rail contact pressure. Further, the longitudinal height profiles of the wing rails and crossing nose are optimised to minimise an estimate of the accumulated damage in the transition zone. The optimisation is computationally efficient which makes it possible to account for very large samples of wheel profiles. An investigation and demonstration of the constraints imposed on the crossing design by the spread in profile and lateral displacement of passing wheels is presented.

Supplementary to the optimisation studies is the comparison of simulation results to field measurement data to evaluate and validate the accuracy of the utilised model of dynamic vehicle–track interaction, as well as a demonstration of a methodology that simulates rail profile degradation for a given mixed traffic situation.

Keywords: dynamic vehicle–turnout interaction, railway turnout, switch & crossing, wheel and rail wear, optimisation

Preface

The work presented in this thesis has been carried out from September 2008 to February 2014 in the Department of Applied Mechanics at Chalmers University of Technology within the project TS13 “Optimization of Track Switches”. This project forms part of the activities in the Swedish National Competence Centre CHARMEC (CHAlmers Railway MEChanics) with special support from voestalpine Bahnsysteme, Trafikverket and SL.

There are a number of persons who directly or indirectly have contributed to this thesis. First and foremost I would like to express my gratitude towards my supervisor Professor Jens Nielsen whose guidance and seemingly infinite patience in improving my manuscripts have been invaluable for the completion of the thesis. I would like to thank Professor Roger Lundén for employing me and for, together with Professor Anders Ekberg, providing the inspirational research environment that is CHARMEC. Credit is also given to my assistant supervisor Professor Thomas Abrahamsson.

I would like to thank the members of the TS13 reference group; Heinz Ossberger and Erich Scheschy of VAE GmbH, Jan-Erik Meyer and Ralf Krüger of Trafikverket, Mounir Ainholm of SL and Professor Igor Rychlik of Chalmers for their guidance and questions. Ingemar Persson, DESolver AB, has provided generous and patient support with GENSYS modelling and simulation. Dr Arne Nissen, Trafikverket, coordinated the INNOTRACK Eslöv field measurements that gave me a lot of good data to work with.

I would like to thank all of my colleagues on the third floor for providing a pleasant working environment. A special mention goes to my long-time companion Anders T. Johansson without whom I might not have ended up as a Ph.D. student. Jim Brouzoulis, if I had half of your confidence and humour, this thesis would have been titled THE Optimisation of Railway Switches and Crossings. Kalle Karttunen, Peter Torstensson and Xin Li have shared the twists and turns of vehicle dynamics simulations and conferences. It has been a great ride.

Steve Jablonsky is complemented for composing the song *Arrival to Earth* included in the score of the film *Transformers* (2007). It provided me with the final burst of inspiration needed to complete this thesis.

Finally, I would like to thank my parents who have always encouraged me to study, and all of my family for their love and support. I love you. You also seem to think that I should work less. I will. I should just finish this first.

Göteborg, February 2014

Björn Pålsson

Thesis Contents

This thesis consists of an extended summary and the following appended papers:

Paper A

A. Johansson, B. Pålsson, M. Ekh, J.C.O. Nielsen, M.K.A. Ander, J. Brouzoulis and E. Kassa, *Simulation of wheel–rail contact and damage in switches & crossings*, *Wear* 271 (1-2) (2010), pp. 472-481

Paper B

B.A. Pålsson and J.C.O. Nielsen, *Wheel–rail interaction and damage in switches and crossings*, *Vehicle System Dynamics* 50 (1) (2012), pp. 43-58

Paper C

B.A. Pålsson and J.C.O. Nielsen, *Dynamic vehicle–track interaction in switches and crossings and the influence of rail pad stiffness – field measurements and validation of a simulation model*. To be submitted for international publication

Paper D

B.A. Pålsson and J.C.O. Nielsen, *Track gauge optimisation of railway switches using a genetic algorithm*, *Vehicle System Dynamics* 50 (S1) (2012), pp. 365-387

Paper E

B.A. Pålsson, *Design optimisation of switch rails in railway turnouts*, *Vehicle System Dynamics* 51 (10) (2013), pp. 1619-1639

Paper F

B.A. Pålsson, *Optimisation of railway crossing geometry considering a set of representative wheel profiles*. To be submitted for international publication

Contributions to Papers

Four of the appended papers were prepared in collaboration with co-authors. The contributions to these papers by the author of this thesis are:

- | | |
|----------------|---|
| Paper A | Took minor part in the planning of the paper
Carried out the simulations of dynamic vehicle–turnout interaction,
and did most of the writing corresponding to this part |
| Paper B | Took part in the planning of the paper
Carried out the numerical simulations
Wrote most of the paper |
| Paper C | Took part in the planning of the paper
Took part in most of the field measurements, but these were
coordinated and performed by Trafikverket and subcontractors
Carried out the numerical simulations
Wrote most of the paper |
| Paper D | Planned most of the paper
Carried out the numerical simulations
Wrote most of the paper |

Contents

Abstract.....	i
Preface	iii
Thesis Contents.....	v
Contributions to Papers.....	vi
Contents	vii
1. Introduction	1
1.1. The railway turnout.....	1
1.2. Motivation of study.....	4
2. Vehicle kinematics in railway turnouts.....	5
2.1. Wheel–rail guidance mechanisms.....	5
2.2. Switch panel kinematics	6
2.3. Crossing panel kinematics	9
3. Vehicle dynamics in railway turnouts.....	12
3.1. Steering.....	12
3.2. Lateral wheel–rail contact forces and wear.....	14
3.3. Vertical wheel–rail contact forces	15
3.4. Conclusions.....	16
4. Turnout rail damage.....	17
5. Literature review of turnout optimisation.....	20
5.1. Switch panel optimisation.....	20
5.2. Crossing panel optimisation.....	21
6. Methods of the project.....	22
6.1. Simulation environment.....	22
6.2. Optimisation algorithms	23
6.3. Latin hypercube sampling.....	23
6.4. Robustness	24
6.5. Comments on methodology	24
7. Summary of appended papers.....	26
7.1. Paper A.....	26
7.2. Paper B.....	26
7.3. Paper C.....	26
7.4. Paper D	27
7.5. Paper E.....	27

7.6. Paper F	27
8. Contributions of the thesis	29
9. Concluding remarks and future work	30
9.1. Methodological comments.....	30
9.2. Implementation	30
10. References.....	32
Appended Papers	35

1. Introduction

The turnout (Switch & Crossing, S&C) is a vital component in railway networks as it provides flexibility to traffic operation by allowing trains to switch between tracks. However, the flexibility comes at a cost as the variation and discontinuities in rail profiles in the switch and crossing panels result in higher rail (and wheel) degradation rates than in regular track.

The work in the present thesis is an effort to optimise the design of railway turnouts. It is focused on the understanding of dynamic wheel–rail interaction in turnouts, and on how the rail degradation can be reduced by optimisation of geometrical and stiffness properties of the track superstructure such as rail profiles, track gauge and rail pad stiffness. The intention is that reduced rail degradation rates will reduce the Life Cycle Cost (LCC) for turnouts.

The investigations are based on simulations of dynamic and kinematic vehicle–turnout interaction. The dynamic analyses are performed using MultiBody Systems (MBS) simulation software. The simulation objective is to reduce rail degradation by improved wheel–rail contact conditions leading to a reduction of wheel–rail contact forces (stresses) and creepages. In order to obtain robust optimised solutions that perform well in traffic, the influence of spread in traffic parameters such as wheel profile and wheel–rail friction coefficient is investigated and accounted for in the optimisations.

In the thesis, methods for optimisation of track gauge and rail profiles in the switch panel and longitudinal height and cross-section profiles of the rails in the crossing panel are presented and demonstrated. Complementary studies are the comparison of simulation results to field measurement data to evaluate and validate the accuracy of the MBS model, and the demonstration of a methodology that simulates rail profile degradation for a given load collective or traffic scenario. This extended summary and the appended papers of this thesis are quite narrowly focused on the project topic of turnout optimisation. For excellent overviews of railway mechanics in general, see for example [1-3]. The work in this thesis is a continuation of the work performed by Kassa within the previous CHARMEC project TS7 [4].

The contents of this thesis summary is organised as follows. In this introductory Section, an introduction to turnouts and a motivation of work are given. Then the kinematic and dynamic consequences associated with the designed rail discontinuities in turnouts are presented in Sections 2 and 3. Section 4 discusses the damage that appears in turnouts due these discontinuities. Section 5 gives a short summary of related work on turnout optimisation. Then the focus switches to the methods, papers and contributions of the present thesis in Sections 6, 7 and 8. Concluding remarks and future work can be found in Section 9.

1.1. *The railway turnout*

There are many different railway turnout configurations to fulfil the needs of varying traffic demands [3, 5, 6]. Figure 1 illustrates a common turnout layout which is studied in the present project. The pictured turnout features a straight section called the through route and a curved deviating part called the diverging route. The front of the turnout is defined as the start of the deviating curve in the switch panel. The switching function is realised by switching machines or actuators that position the switch rails according to the desired traffic route. The closure panel connects the switch and crossing panels, whereas the crossing panel allows for wheels to travel along both intersecting paths. Opposite to the

crossing, and next to the adjacent through (stock) rails, are the check rails that enforce a constraint on the lateral position of passing wheelsets. This is to avoid interference contact between wheel and crossing nose.

Photos of switch and crossing panels can be found in Figure 2 and Figure 3, respectively. In Figure 2 it can be observed that the switch rails are positioned to the left with the left switch rail in contact with the left stock rail to catch the wheel flange, while the right switch rail is positioned away from the right stock rail to allow wheels to pass through on the stock rail. The methods and analyses presented in this thesis have been developed using a common Swedish turnout type denoted 60E1-760-1:15. The designation means that the turnout is based on 60E1 rails, has a constant 760 metre radius without transition curves and a turnout angle of 1:15. The turnout angle is the angle between the straight and diverging tracks. The switch rails are of the flexible type and are milled from dedicated switch rail specimens with a lower height and a thicker and asymmetrical rail foot compared to standard rails. The crossing designs studied are of the fixed type which means that they passive rail components that cannot be operated.

For some traffic types, such as for very high axle loads or high vehicle speeds, movable crossing noses are used [3]. This type of crossing is utilised to avoid the large damage inducing discontinuity in the rail associated with a fixed crossing. While the results presented here are for a particular turnout configuration, the methods can be readily applied also to other turnout designs with different rail profiles, radii and turnout angles.

The variations and discontinuities in rail profiles, present in the turnout to achieve the function of the switch and crossing, result in an increased dynamic loading during wheel passage and thus increased degradation of these components compared to regular track. Details of the discontinuities in the switch and crossing panels can be studied in Figure 4. Further, turnouts are often built without transition curves, causing high vehicle jerk (time derivative of lateral vehicle acceleration) at entry and exit of the diverging route. Due to the planar nature of a turnout, track inclination (cant) to compensate for the lateral acceleration is not possible.

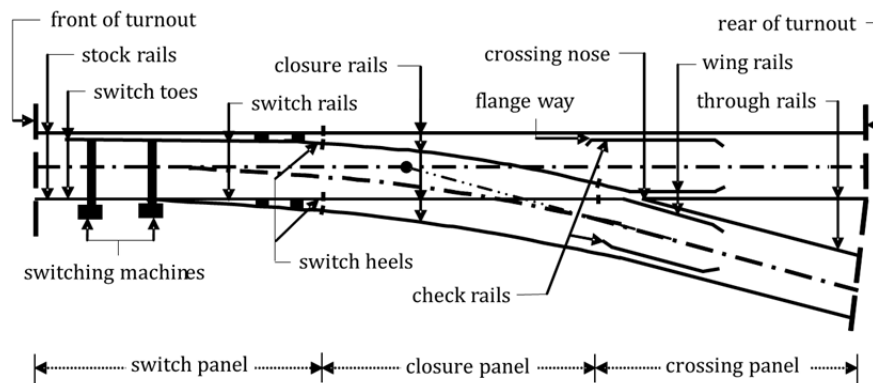


Figure 1. Schematic illustration of a turnout and its components



Figure 2. Overview of switch panel from the front of the turnout including switch rails and switching machines



Figure 3. Overview of crossing panel from the rear of the turnout including a fixed crossing and check rails



(a) (b)
Figure 4. Details of (a) switch rail and stock rail, (b) fixed crossing

1.2. Motivation of study

There can be many reasons for applied research, but the motivations are typically economical. Applied research can be considered as a (risky) investment that can pay off in the form of improved design concepts or methods of economic value. The expected return on this investment is thus dependent on the costs involved and the potential for improvement. In the case of railway turnouts, the costs are high as they constitute a key component in railway systems all over the world and consume large capital resources for their construction and maintenance. Even though the concept of railway turnouts is old, it will be argued in this thesis that there is room for improvement in their design and practical implementation. Especially as the published body of knowledge on turnout geometry optimisation is not very large as can be seen in Section 5.

Turnouts stand for a considerable contribution to reported track faults. Only in Sweden there are over 12 000 turnouts in some 17 000 km of track [7], and the cost for turnout operation and maintenance was 250 – 300 MSEK per year in 2001 to 2004 [8].

In the EC FP6 sponsored European project INNOTRACK [9], LCC models were used to find cost drivers for switches and crossings and to study the cost benefits of innovative solutions.

Within INNOTRACK, Deutsche Bahn (DB) analysed a set of 458 turnouts on a high speed line with a mixed traffic volume of about 17.5 mega gross tonnes (MGT) per year [10]. It was concluded that 50 % of the overall costs were for inspection, service and test measures. Out of the remaining costs it was found that renewal of switch rails, crossings and large elements such as check rails stood for 65 % of the costs while other maintenance activities such as welding and tamping constituted the remainder of the costs. With such a large contribution to the overall costs, it was quite naturally found that optimised components such as switch rails and crossings with a longer service life can help to reduce the life cycle costs for turnouts [9]. See also [7] for the application of LCC-analysis to S&C.

2. Vehicle Kinematics in Railway Turnouts

As a motivation and background for the focus on turnout geometry optimisation in this thesis, the kinematical challenges for a railway vehicle in the switch and crossing panels will now be presented in more detail. The section on switch kinematics is based on the investigation carried out for **Papers D** and **E**, while the section on crossing kinematics is based on the work for **Paper F**. First a brief introduction will be given to wheel–rail guidance mechanisms.

2.1. Wheel–rail guidance mechanisms

To better understand the geometrical or kinematic situations encountered when a wheel passes through an S&C, a short introduction to wheel–rail guidance mechanisms will be given inspired by the presentation in [1]. Figure 5 illustrates the contact conditions for a wheelset with S1002 wheel profiles at two different lateral displacements on nominal 60E1 rails. The dashed wheel profiles illustrate the situation where the wheels are positioned on the rails with zero lateral wheelset displacement, $\Delta y = 0$, whereas the wheel profiles drawn with full lines correspond to a situation where the wheelset is displaced outwards, $\Delta y > 0$. Due to the conical shape of the wheels, the lateral and vertical locations of the wheel–rail contact points will change when the wheelset is displaced laterally, in particular for the right wheel which in this case is displaced towards the rail gauge corner and where the contact point is located on the wheel flange.

Also due to the conical shape of the wheels, the effective rolling radius for each wheel will change as the contact point location changes. This phenomenon can be illustrated using a rolling radius difference diagram as shown in Figure 6. Here the difference in rolling radius between the left and right wheels is illustrated as a function of lateral wheelset displacement. As the wheels in a standard wheelset are rigidly connected via an axle, the rolling radius difference provides a counteracting steering effect as the wheel with the larger rolling radius will travel faster for a given rotational speed of the wheelset. A non-dimensional measure of the influence of lateral wheelset displacement on the difference in rolling radius, and thus steering, is obtained by the concept of equivalent conicity as shown in Equation (1).

$$\lambda_{eq} = \frac{r_r - r_l}{2\Delta y} = \frac{\Delta r_r - \Delta r_l}{2\Delta y} \quad (1)$$

Here r_r/l are the rolling radii of the left and right wheels and Δ indicates a change. Note that the rolling radius difference is typically a non-linear function of the lateral displacement, as exemplified in Figure 6, which makes λ_{eq} a linearized measure that is only valid for a given lateral displacement amplitude.

If the equivalent conicity is low over a range of lateral rail and wheelset displacements, these movements will have a small impact on the steering and the resulting lateral displacements of the wheelset, while a higher equivalent conicity will induce more steering and larger motions. Further discussions on equivalent conicity and its connection to steering and running stability can be found in e.g. [1, 2].

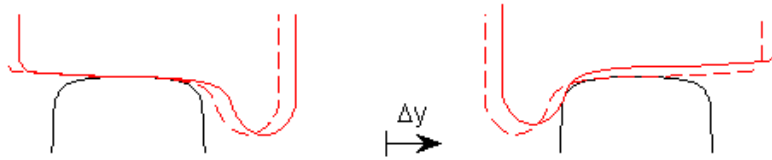


Figure 5. Illustration of vertical wheel movement and change of rolling radius with lateral wheelset displacement Δy . The lateral rail and wheel spacing is not to scale

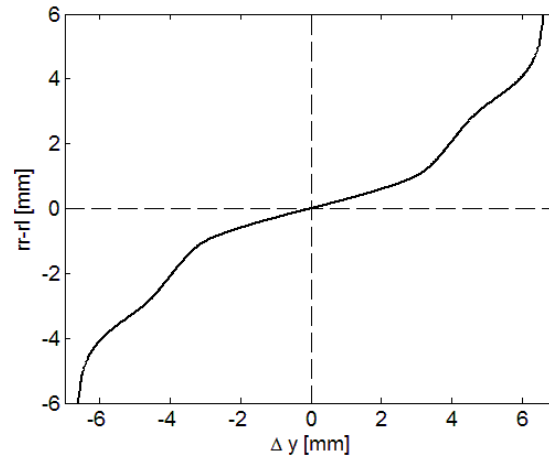


Figure 6. Rolling radius difference as a function of lateral wheelset displacement. Results for a nominal S1002 wheel on nominal 60E1 rails without inclination

2.2. Switch panel kinematics

A set of nominal composite rail profiles representing the switch and stock rails in the switch panel is shown in Figure 7. Due to the discontinuity at the separation between the deviating stock rail and the straight switch rail as seen in the figure, the rolling radius difference ($r-r$ difference) curve is non-smooth in some areas. This can be observed in Figure 8, which shows the rolling radius difference in a contour plot as a function of wheelset position from the front of the turnout and lateral wheelset displacement Δy . The figure is based on the rail geometry in Figure 7 with an added nominal rail profile on the opposite side. The configuration is thus the same as in Figure 5 but with one nominal rail replaced by the switch rail cross-sections from Figure 7. Before the calculation of rolling radius difference, all cross-sections were positioned to achieve nominal track gauge (lateral rail spacing) for the switch panel. The wheel profile used is a nominal S1002 wheel profile and the rolling radius difference characteristics were calculated using GENSYs [11]. Note that only lateral wheelset movement towards the switch rail is considered here, but that Figure 8 is applicable for traffic in both the through and diverging routes.

Compared to the rolling radius difference characteristics obtained for a pair of standard 60E1 rails, which is visible in the diagram beyond 10 m, the composite profile combinations cause kinematic problems along most of the tapered switch rail that affect traffic in both the through and diverging routes.

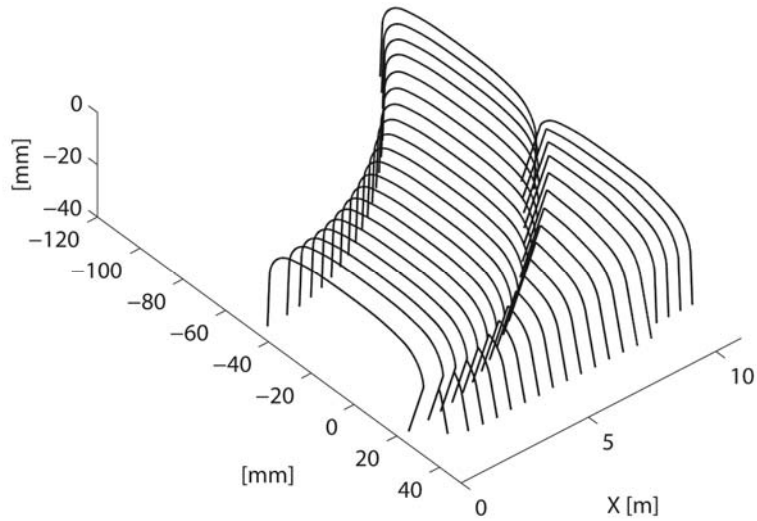


Figure 7. Nominal switch rail sections where X is the distance from the front of the turnout

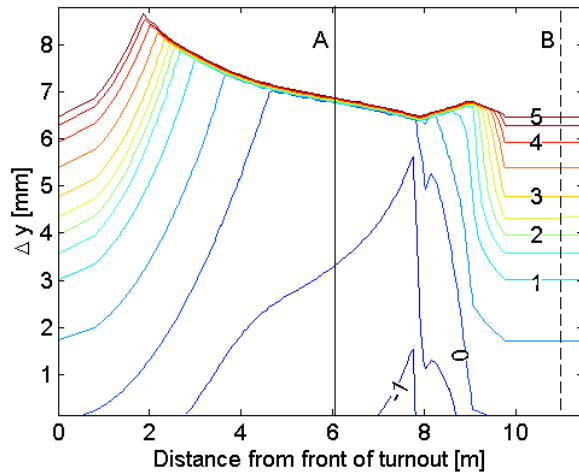


Figure 8. Contour plot of rolling radius difference [mm] as a function of lateral wheelset displacement towards the switch rail and position from the front of the turnout. The plot is based on the rail geometry in Figure 7 and a nominal S1002 wheel profile

The difference in rolling radius difference characteristics between sections can be studied in more detail in Figure 9. Here the rolling radius difference for the two cross-sections A and B in Figure 8 are plotted. It can be noted that the rolling radius difference characteristics at cross-section B, where there is a nominal 60E1 profile, is smooth and progressive and goes to zero for zero wheelset lateral displacement. This indicates that the rolling radius difference characteristics are symmetrical as can be expected when the rail profiles are the same on both sides as in Figure 6. At cross-section A, however, there is a rolling radius difference at $\Delta y = 0$ indicating an asymmetrical rail configuration. Then there

is a small linear increase until the wheel flange makes contact with the switch rail leading to an abrupt increase in rolling radius difference. As this situation corresponds to flange climbing, it will typically not appear during normal negotiation of a switch. Instead the wheel will be subjected to a two-point contact situation with one contact point on the switch rail and one on top of the stock rail. The asymmetric rolling radius difference characteristics in the switch panel also make the wheelset steer towards the switch rail even if the track is straight as in the through route, as there is a negative rolling radius difference towards that side due to the deviating curved stock rail.

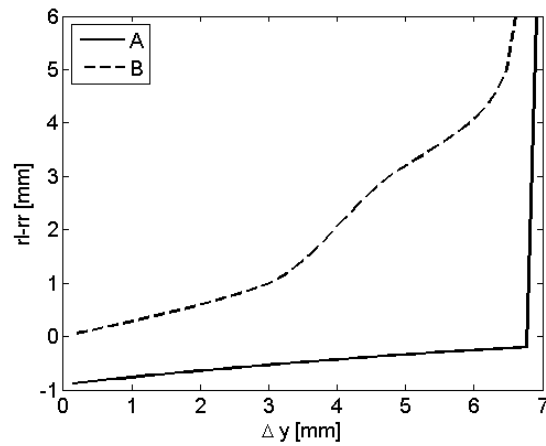


Figure 9 Rolling radius difference characteristics for sections A and B of Figure 8

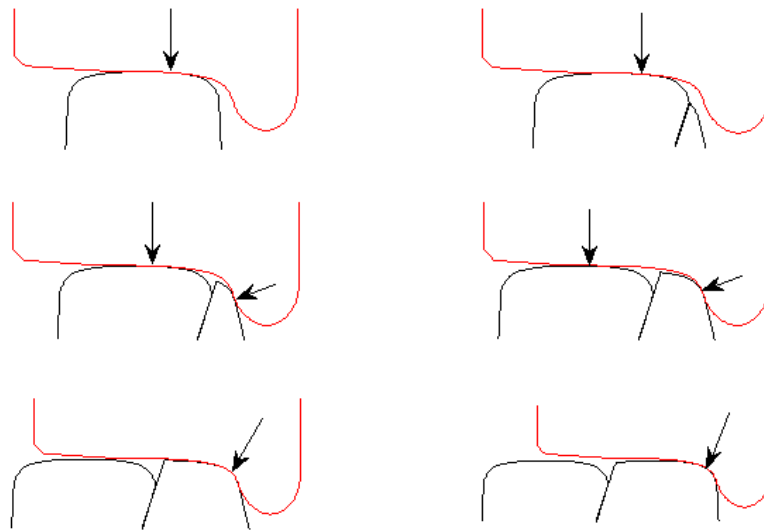


Figure 10. Schematic contact conditions and normal wheel-rail contact forces during a switch transition in the diverging route

A schematic presentation of the contact conditions when a wheel passes through the switch in the diverging route is presented in Figure 10. As the wheel is travelling on the outside rail of the turn it has to generate a lateral wheel–rail contact force. Due to the poor conicity properties related to the composite switch rail cross-sections, the wheel ends up in the above described two-point contact situation which causes poor steering and significant amounts of wear as the difference in rolling radius between the contact points induces relative motion between wheel and rail in the contact points. A mitigation of the rolling radius difference asymmetry using prescribed track gauge widening in the switch panel is studied in **Paper D**. How the switch rail profile design can improve the rolling radius difference characteristics in the switch panel is studied in **Paper E**.

2.3. Crossing panel kinematics

A fixed railway crossing constitutes another kinematic challenge in terms of the wheel–rail contact. The fact that two different rail and wheel paths intersect at one point requires that there exist flangeways which allow for the wheel flanges to pass through the crossing. Therefore the rails are split into a crossing nose and two wing rails. The layout for the crossing panel can be studied in Figure 1 and a detailed top-view of the crossing layout is presented in Figure 11.

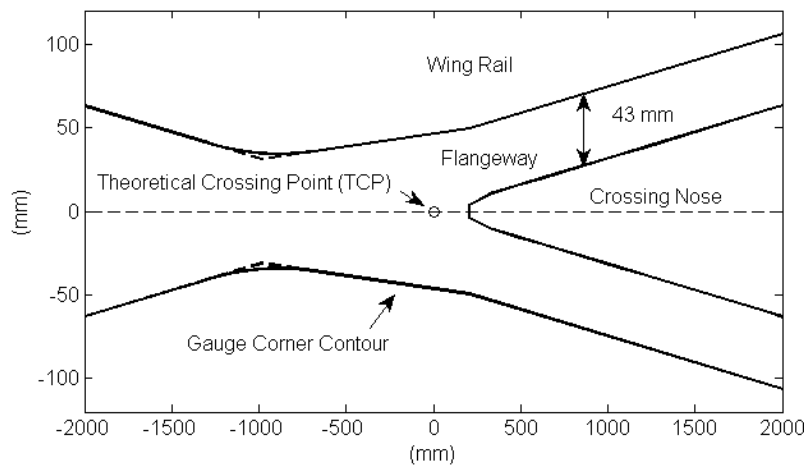


Figure 11. Top view of gauge corner contour at crossing

When a wheel passes over the crossing in the facing move (from the switch panel towards the crossing panel) it will first encounter the wing rail. Due to the outwards deviation of the wing rail, the wheel–rail contact point will move towards the outside of the wheel profile. For a typical conical wheel profile, the rolling radius will decrease and the wheel will move downwards unless the wing rail is elevated. The reduced rolling radius on the crossing side will induce a yawing motion of the wheelset towards the crossing. Due to the check rail, the lateral motion of the wheelset is restrained and wheel flange interference contact with the crossing nose is prevented.

When the wheel reaches and makes contact with the crossing nose, the contact load is quickly transferred from the wing rail to the crossing nose. For a typical conical wheel profile, the rolling radius increases as the new contact point is close to the flange root. The

two-point contact situation during the transition with contacts at different rolling radii induces relative tangential motion in the contacts that causes wear. The transition typically also results in a significant impact force on the crossing nose (or the wing rail depending on the traffic direction) as the slight downward motion of the vertical wheel trajectory is reversed and the wheel is accelerated upwards by the crossing nose. Using eight cross-sections along the crossing, a schematic illustration of the crossing transition for a single wheel profile is illustrated in Figure 12. The vertical wheel positions at the different sections that form the vertical wheel trajectory are shown in Figure 13.

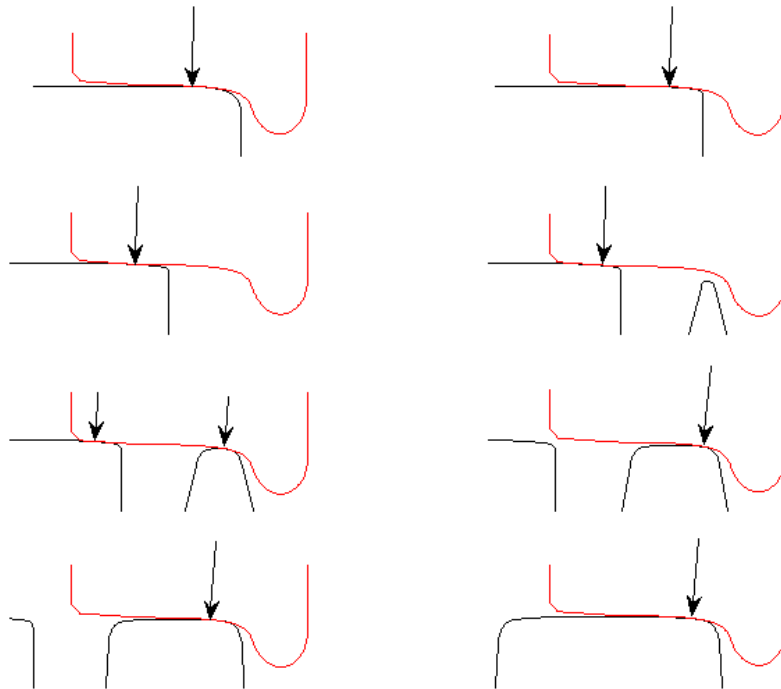


Figure 12. Schematic contact conditions and normal wheel-rail contact forces during a crossing transition

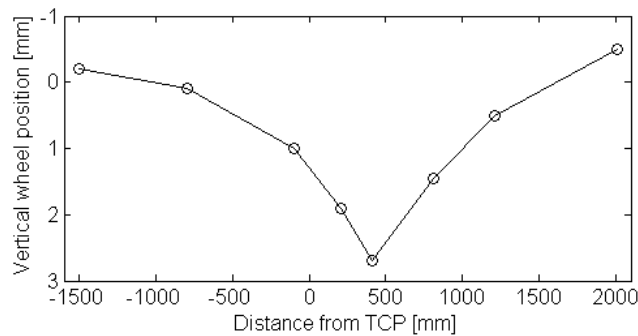


Figure 13. Vertical wheel trajectory, based on vertical wheel positions corresponding to the cross-sections of Figure 13, as a function of distance from the Theoretical Crossing Point (TCP)

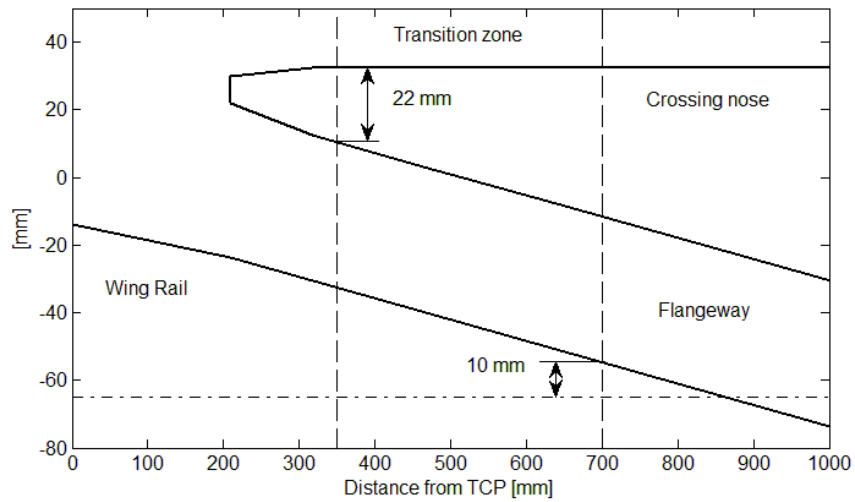


Figure 14. Top view of crossing geometry with crossing angle 1:15. TCP = Theoretical Crossing Point

Figure 14 shows a schematic top view of a fixed crossing oriented along one of the traffic directions. The wheels pass over the crossing in the horizontal direction in the figure and the horizontal dash-dotted line indicates the nominal position of the outer side of the wheel. The vertical dashed lines indicate the beginning and end of the transition zone. The exact extension of the transition zone can vary, but it can be concluded that wheels should not make contact with the crossing nose where it is too thin to carry the wheel load, and they should not make contact with the wing rail where the overlap between wheel and wing rail is too small to provide satisfying contact conditions. These parts are marked with stripes in the figure. Thus, there is a given (short) distance where it is preferred that passing wheels make their transition from wing rail to crossing nose or from crossing nose to wing rail. The implications of a limited transition zone and varying geometry of the passing wheel profiles and the constraints these set for crossing geometry design are investigated further in **Paper F**.

3. Vehicle Dynamics in Railway Turnouts

To illustrate some of the implications of the turnout rail discontinuities discussed in Section 2 on dynamic vehicle–turnout interaction, the vehicle dynamics for two simulation cases will be compared using the model from **Paper C** where a 60E1-760-1:15 turnout is studied. The first case consists of a simulation where a freight vehicle negotiates a turnout in the facing move of the diverging route. The second case is a fictitious case using the same configuration as the first, but the turnout rail profile geometry has been replaced by a nominal 60E1 rail with constant cross-section throughout the turnout. The track in the second case is thus a constant radius curve without transition curves, no rail inclination and no cant. The check rail is still in place. The difference in vehicle dynamics for the two cases will be discussed in subsections on different themes. In the graphs, the tapered part of the switch rails are roughly located between 0 to 10 m from the front of the turnout and the crossing transition takes place at around 47.3 m as indicated by the vertical dashed line.

3.1. Steering

Figure 15 presents a comparison of simulated yaw rotation for the leading wheelset relative to the radial position (an orientation normal to the track centreline) for the two cases. A negative yaw angle means that the wheelset is oriented such that it strives to steer out of the turn. It is clear that the standard rail profile provides a better steering capability in the beginning of the curve as the maximum rotation amplitude is smaller and the wheelset reaches a steady-state orientation earlier for this case. Further understanding of this phenomenon can be gained from Figure 16, where the wheelset yaw moment is presented for the same cases. It can be observed that in the simulation featuring a constant rail cross-section a much larger yaw moment is generated after the vehicle has entered the curve.

At the crossing, the wheelset is moved laterally towards the inside of the turn when it comes into contact with the check rail as can be observed in Figure 17. The rolling radius difference is therefore reduced (see Figure 6 when the Δy magnitude decreases) leading to a reduced yaw moment for both simulation cases as can be seen in Figure 16 and accordingly a reduced yaw angle as shown in Figure 15. The more aggressive outward turn at the crossing for the simulation with turnout rails is due to the interaction with the wing rail which reduces the rolling radius of the outer wheel even further compared to the case with the nominal rail. For the case with turnout rails, the torque is even reversed due to the reduction in rolling radius that appears when the outer wheel travels on the wing rail and the contact point moves towards the outside of the wheel. The yaw moment increases again after the crossing transition (indicated by the vertical dashed line) as the rolling radius of the outer wheel is larger when it is in contact with the crossing nose.

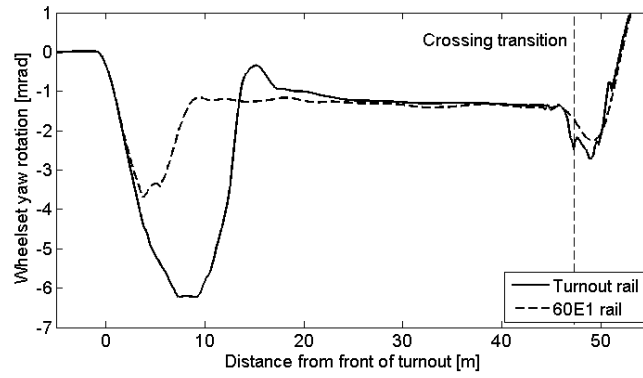


Figure 15. Yaw rotation of leading wheelset (positive yaw in the direction of the curvature). Nominal turnout rail geometry is compared to a fictitious case with a constant 60E1 rail cross-section

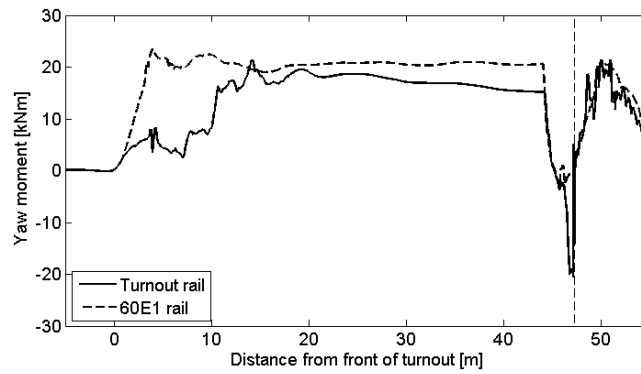


Figure 16. Yaw moment on leading wheelset (positive moment on wheelset in the direction of the curvature). Nominal turnout rail geometry is compared to a fictitious case with constant 60E1 rail cross-section

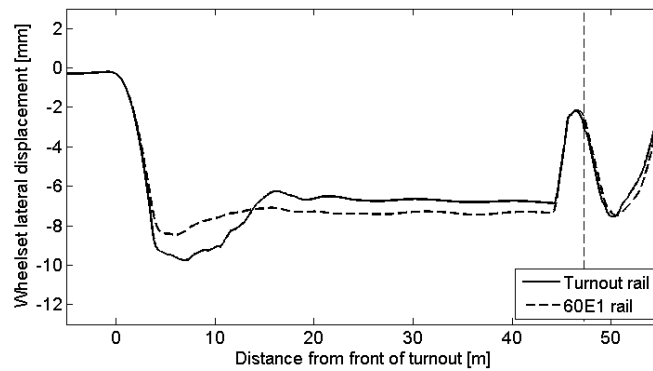


Figure 17. Lateral displacement of leading wheelset (positive towards the inside of the turn). Nominal turnout rail geometry is compared to a fictitious case with a constant 60E1 rail cross-section

3.2. Lateral wheel–rail contact forces and wear

The total lateral wheel–rail contact force acting on each wheel of the leading wheelset in the two simulation cases can be seen in Figure 18. The contact forces on the wheels are positive when acting towards the track centre. This means that the contact forces push the left and right wheels towards each other when they pass through the switch panel, and away from each other during the crossing transition. The lateral contact forces in the switch panel and at the crossing transition point are much larger for the simulation case with turnout rails. The large contact forces in the switch panel are associated with the poor steering performance presented in Figure 15 and Figure 16 and the force peak at the transition point is due to the impact force on the crossing nose. The sudden reversal of the lateral contact forces during the crossing passage is due to the wheelset’s interaction with the check rail and is thus present for both simulation cases.

Further evidence that the counteracting lateral contact forces during the switch and crossing transitions are a kinematic phenomenon can be found in [12]. In that study, lateral contact forces in the diverging route of a turnout of the same type as investigated here were measured at vehicle speeds 80 and 10 km/h. Comparing the two measurements, there was a relatively small difference in the lateral contact forces for the two vehicle speeds. This indicates that the large contact forces are due to the constraining kinematics as it can be anticipated that the dynamic contribution to the contact forces is small at 10 km/h. For example, the vertical impact force at the crossing vanishes at 10 km/h.

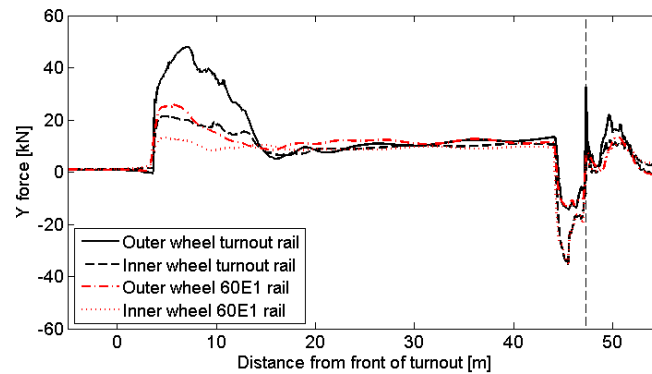


Figure 18. Total lateral wheel–rail contact force acting on inner and outer wheels. Positive force on wheel is directed towards track centre. Nominal turnout rail geometry is compared to a fictitious case with constant 60E1 rail cross-section

The energy dissipation, or friction work in the wheel–rail contacts, for each wheel during a switch passage is shown in Figure 19. The energy dissipation for each contact patch is calculated as $W = F_x \vartheta_x + F_y \vartheta_y + M_z \varphi$, [1], where $F_{x/y}$ are the creep forces in the contact patch plane, $\vartheta_{x/y}$ the corresponding creepages and M_z the spin moment and φ the spin. The energy dissipation can also serve as a (non-linear) estimate of wear and RCF [1, 13, 14]. It can be noted that the W -values are much larger for the turnout rail geometry during the switch transition. This is because of the situation with two contact points at different rolling radii for the outer wheel during the switch passage as illustrated in Figure 10. This contact situation is associated with a large creepage in the flange contact. The difference between the two simulation cases is not very large during the crossing

transition, but the W -values are slightly higher for the turnout rail when the wheel is in contact with the wing rail and at the transition point.

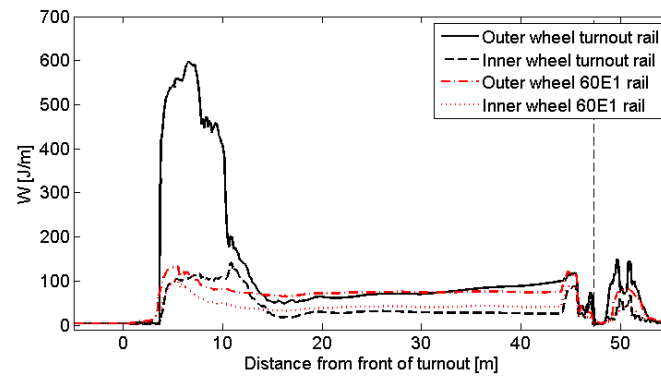


Figure 19. W (energy dissipation) during a turnout passage for two simulation cases with different rail configurations

3.3. Vertical wheel–rail contact forces

As the stock rail to switch rail transition has very small gradients in the vertical direction, the vertical dynamics is typically not significant during the switch passage. However, the dip (impact angle) in the vertical wheel trajectory during the crossing passage as exemplified in Figure 13 typically causes a significant impact force as illustrated by the simulated vertical contact forces Q shown in Figure 20. The difference in vertical contact forces throughout the turnout between the inner and outer wheels is due to the load transfer, or overturning moment on the vehicle, caused by the centripetal acceleration in the curve.

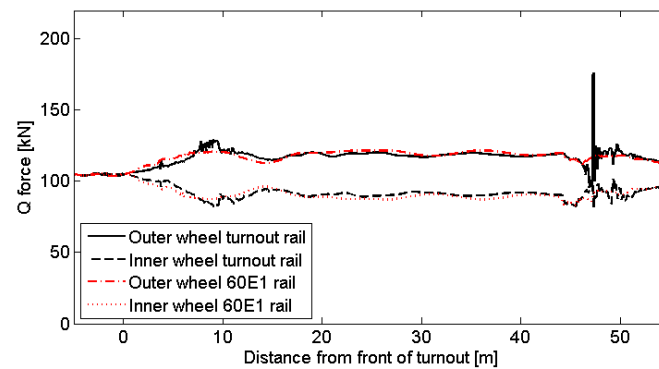


Figure 20. Vertical wheel–rail contact force Q for the leading wheelset in the facing move of the diverging route

3.4. Conclusions

The conclusion drawn from these two simulation cases is that there is potential for reduction of lateral wheel–rail contact forces in the diverging route if the conditions of rolling radius difference or conicity conditions throughout the turnout can be improved. The magnitudes of the lateral wheel–rail contact forces are typically quite low in the through route, but there can be some wear during the stock rail to switch rail transition as investigated in **Paper D**. Otherwise the impact force at the crossing is the most important problem in the through route as the vehicle speeds typically are higher in the through route compared to the diverging route. The possibilities to optimise the crossing geometry for reduced impact forces are investigated in **Paper F**.

4. Turnout Rail Damage

A review of typical rail damage mechanisms in turnouts was conducted in [6]. The damage mechanisms observed in turnouts are mechanical contact damage such as wear, plastic deformation, (rolling contact) fatigue and fracture. As presented in Section 3, the rail discontinuities in the switch and crossing panels increase the wheel–rail contact forces compared to standard rails, while the rail cross-sections that carry the load are weaker (i.e. smaller rail head cross-section area) than for standard rails. More severe damage and faster degradation rates can therefore be expected for the rails in switches and crossings.

Examples of turnout rail damage can be observed in the pictures below. In Figure 21, a piece of the switch rail has been broken off due to a fatigue crack that has propagated horizontally just below the top of the switch rail. Figure 22 shows a manganese-steel crossing where material has been lost due to spalling. Spalling damage occurs when surface initiated cracks propagate under the rail surface until a piece of material comes loose. Figure 23 shows a crossing nose that is too low as material has been removed due to wear and relocated due to plastic deformation. For a thorough discussion of wheel–rail interface phenomena such as rail damage, see for example [15]. The crossing transition may also cause significant wear and damage on the wheels [16].

As the geometry of a turnout degrades, the contact conditions for the passing wheels may become worse and the deterioration rate can increase, thus creating a self-reinforcing spiral with an increasing degradation rate. An example of increased forces due to geometry degradation can be taken from the Dutch railways: In [17], the effect of crossing geometry degradation on the impact force during the crossing transition has been verified experimentally. By placing an accelerometer on a crossing and mounting sensors to detect passing wheels beside it, it was possible to determine the wheel position associated with the maximum vertical acceleration of the crossing.



Figure 21. Worn switch rail where a crack has grown from the rail head down into the material, propagated longitudinally and finally turned upwards again causing the removal of a large part of the switch rail. From [6]

Assuming that the position of the maximum acceleration corresponds to the position and magnitude of the impact force on the crossing, it was possible to investigate the characteristics of the impact forces before and after geometry maintenance of the crossing. In this example it was found that the transition points were more distributed after geometry correction of the crossing, and that on average the magnitudes of the forces (accelerations) were reduced by a factor of 1.7. The relation between force and acceleration should be the same before and after grinding as no system stiffnesses, such as pad stiffness, were changed.



Figure 22. Spalling (loss of material chips) on a manganese steel crossing nose. From [6]



Figure 23. Worn crossing nose as shown by the vertical distance between template and crossing nose. From [6]

The present project aims to reduce the degradation of turnout rails, but it should be remembered that quantitative estimates of rail degradation is a very complex task that requires large computing power as demonstrated in [18] and **Paper A**. Therefore, in an optimisation where a computationally inexpensive evaluation of the objective function is vital, the damage estimates have to be formulated in more qualitative terms using wheel–rail interaction quantities such as lateral or vertical contact force, creep and contact pressure. Examples of such criteria are maximum normal contact force, energy dissipation in the contact patch or indices for RCF initiation such as FI_{surf} [19].

5. Literature Review of Turnout Optimisation

As mentioned in the introduction, the focus of this thesis is geometry and stiffness optimisation of railway turnouts. To set the present work into context, previous research in the area will be discussed for the switch and crossing panels.

5.1. *Switch panel optimisation*

Kinematic gauge optimisation (KGO), or Fahrkinematische Optimierung (FAKOP), is a design solution marketed by the Austrian company VAE GmbH [20]. In short, the idea is that a prescribed anti-symmetric gauge widening in the switch panel can compensate for the asymmetric rail profile configuration associated with the closed switch rail as discussed in Section 2.2. It has been shown by simulations that this is an efficient approach to decrease wheel–rail contact forces and wear in the switch panel, see [21–24]. All of these studies were performed using multibody simulations of some sort. The work in **Paper D** supports these findings.

In [21], results are presented which show that the FAKOP design and the use of clothoid curves (curves with a linear variation of curvature) instead of constant radius curves can significantly reduce the wheel–rail contact forces in the switch panel. In [22], a FAKOP turnout geometry and a standard turnout geometry are compared for four different wheel profiles. Again, it is shown that the FAKOP design leads to a reduction in wheel–rail contact forces. Studying the lateral wheelset displacement in the through route, it was (as can be expected) demonstrated that the gauge clearance and the conicity of the wheel profiles affect the amplitude and wavelength of the lateral wheelset movement and consequently the wheel–rail contact forces. It should be noted that in the above studies the commercial FAKOP design was investigated. Thus, no specific details regarding the applied gauge widening or switch panel design were disclosed.

In [23], two different principles for wheelset guidance in the switch panel are discussed, FAKOP and CAFTERSAN. In the CAFTERSAN solution the height of the inner part of the rail crown of the stock rail is reduced such that the wheel–rail contact point is moved outwards. In this way a reduction of rolling radius is obtained and a FAKOP-like effect is obtained without increasing the actual track gauge. The paper also discusses the importance of the height of the switch rail in the facing move of the through route. It is shown that if the switch rail height is increased, the wheel will make the full transition to the switch rail at a position closer to the front of the turnout. If the transition appears earlier in the switch panel, there will be less distance for the wheelset to move laterally due to the asymmetric rail profile configuration. Therefore the lateral speed of the wheelset will be lower before the transition from stock rail to switch rail, and therefore also the impact forces and wear during the transition will be lower. To make an earlier transition feasible, it is pointed out that the strength of the switch rail is important. This work is closely related to the switch rail optimisation presented in **Paper E**.

In [24] and [25], gauge optimisation studies from the INNOTRACK project are presented. The introduced gauge widening is bell-shaped, and all details regarding the geometry are disclosed. For a range of wheel profiles, it is found that the gauge widening is effective in reducing the wear during the stock rail to switch rail transition in the through route. However, the investigated gauge widening shape did not produce a significant reduction of damage in the diverging route.

5.2. *Crossing panel optimisation*

INNOTRACK studies on crossing optimisation by simulations in the commercial MBS code SIMPACK are presented in [25] and [26]. Both stiffness and geometry optimisation studies were undertaken. It was found that a reduction of rail pad stiffness (resilient layer between rail and sleeper) could significantly reduce the impact forces during the crossing transition. Optimisation of the crossing geometry was performed by the assessment of different crossing designs for three wheel profiles at different states of wear. It was concluded that it is very difficult or even impossible to design a crossing geometry that provides an impact force reduction for all wheel profiles that occur in service, but no formal investigation of this constraint was given. An effort to provide such an analysis is presented in **Paper F**. In the INNOTRACK studies, however, the so called MaKüDe design showed the best performance. Also in the INNOTRACK literature [27], a kinematic tool for the investigation of vertical wheel trajectories over the crossing for a range of lateral wheelset displacements is presented.

In [28], the influence of track stiffness on the wheel–rail impact force on the crossing nose is studied using a two-dimensional MBS model. It was found that the impact force can be significantly reduced by introducing a more resilient track structure. Based on analytical studies of the impact dynamics at a track dip, it is an expected result (depending on the frequency spectrum of the induced load) that a reduced pad stiffness can reduce the magnitudes of the impact force [1, 29]. In relation to these studies, the influence of rail pad stiffness is investigated experimentally in **Paper C**.

An automated optimisation using a parameterised crossing nose geometry is described in [30], where the crossing designs are evaluated by MBS simulations using one wheel profile. A multi-objective formulation with respect to wear index and wheel–rail contact pressure was used for the optimisation. It was found that an altered shape of the crossing nose reduced the objective quantities. The robustness of the optimised solution was investigated by the introduction of different initial disturbances of the wheelset before the crossing transition and different track conditions. A related parameter study on crossing nose geometry is presented in [31]. The longitudinal height profile of a movable crossing nose is optimised in [32].

6. Methods of Study

In the present project, the focus is on the optimisation of the dynamic wheel–rail interaction as influenced by the geometry of the turnout. This section will give an overview of the different methodologies chosen to address the task of robust turnout geometry optimisation.

6.1. *Simulation environment*

The tool chosen for the investigation of dynamic vehicle–turnout interaction is numerical multibody simulations (MBS). The method of multibody system dynamics considers systems of interconnected rigid and deformable bodies that undergo large translational and rotational displacements [33]. The method is chosen as it is a computationally efficient method to obtain relatively accurate results for the dynamic interaction in a vehicle–turnout system including the kinematics of the interacting parts and the corresponding interaction forces. This is especially important in an optimisation setting where fast simulation times are of essence. As has been presented in Section 5, multibody simulation tools are popular for simulations of dynamic vehicle–turnout interaction. For a detailed mathematical treatment of multibody dynamics formulations in a railway setting, see for example [34]. For an introduction to the topic and the practical application of multibody simulations in a railway environment, see for example [1, 2].

The MBS simulations have been performed using the software GENSYNS [11], which is a general MBS software that is specialised in dynamic vehicle–track interaction. The vehicle–turnout interaction has mainly been investigated for freight traffic using a simulation model of a vehicle with the common Y25 bogie that was developed in [35]. In **Paper D**, the dynamic interaction between a Regina passenger train and the switch panel was also studied.

In the model, the track is represented by co-following mass–spring–damper systems that are coupled to each wheelset in the vehicle model (moving track model). For each combination of wheel profile and sampled rail cross-section, and for a range of prescribed lateral displacements of the wheel position relative to the rail, the wheel–rail contact geometry problem is solved in advance using the GENSYNS module *kpf* which fits an equivalent Hertzian model to the contact conditions. Using a linear interpolation procedure, the tabulated contact geometry functions are then used in the subsequent time integration analysis. Hertzian contact theory [36] is used to obtain a linearised normal contact stiffness. The tangential contact problem is solved using the FASTSIM algorithm (simplified theory according to Kalker [37]). The contact model accounts for two-point contact situations.

The mathematical computing software Matlab [38] has been used for pre- and post-processing purposes. In **Papers D, E and F**, Matlab was also used to operate the optimisation loops. In an optimisation loop, input data files for GENSYNS are automatically generated in each iteration of the optimisation as a function of the design variables that prescribe the shape of the parameterised rail geometries. Then GENSYNS is started from Matlab using the *system* command. When the simulations are completed the objective is calculated based on the simulation results and fed into the optimisation algorithm. The optimisation algorithm supplies a new set of design variable values and the process starts all over again.

6.2. Optimisation algorithms

Genetic or evolutionary type algorithms have been used for the optimisations in this thesis. The motivation for using this type of algorithm is that it is relatively robust and suitable when analytical expressions of the objective function and its derivatives are not available. As the objective criteria in this project are calculated from output data from numerical simulations, the objective function is not available in analytical form. Due to the “black box” situation, it is impossible to prove that the minimum objective found in an optimisation is actually the global minimum. Instead the optimisations are verified by performing repeated optimisations and checking that the utilised genetic algorithm converges to the same (within some tolerance) solution each time, when starting from different initial populations. Due to the random nature of genetic algorithms, their exact optimisation history is not repeatable. A drawback of evolutionary algorithms is slow convergence.

Evolutionary algorithms are especially suitable for multi-objective optimisation problems, see **Paper D** and **Paper E**, as they can solve such problems in a single run. The specific algorithms used are Matlab’s *ga* for single-objective optimisation and *gamultiobj* for multi-objective optimisation. The *gamultiobj* algorithm is based on the NSGA-II algorithm presented in [39, 40]. For an excellent introduction to biologically inspired optimisation methods, see [41].

6.3. Latin hypercube sampling

In this project, the Latin Hypercube Sampling (LHS) method [42] has been used to generate samples of randomised vehicle input data for the simulations. The parameter types concerned are for example wheel–rail friction coefficients and wheel profiles. The LHS method is a variance reducing technique used to guarantee a certain spread in each individual sample. If the samples are generated completely at random as in a standard Monte Carlo method, there is no such guarantee. All the sampling points could, even though unlikely, come from one end of the probability distribution for the parameter in question. The correlation between geometry characterisation parameters for wheel profiles and damage in S&C is studied in **Paper B** in order to find the parameter that correlates best to damage. This parameter can then be used to rank the wheel profiles in the Latin Hypercube Sampling, and the variance in properties between different wheel profile samples can be reduced which in turn reduces the variance in the calculated objectives.

The sampling methodology of the LHS method involves a basic sampling matrix \mathbf{S} calculated as, [42],

$$\mathbf{S} = \frac{1}{N}(\mathbf{P} - \mathbf{R}) \quad (2)$$

The matrices \mathbf{P} and \mathbf{R} have dimensions $N \times K$, where N is the sample size and K is the number of stochastic vehicle input variables. In \mathbf{P} , each column is a random permutation of the numbers 1 to N , and in \mathbf{R} each element is an independent random number from the uniform distribution (0,1). Each column of \mathbf{S} contains N elements from N bins of equal size with values between 0 and 1. Due to this construction of the \mathbf{S} matrix, the values are random, but there is exactly one value from each bin along the uniform distribution. Some parameter spread in each sample is thus guaranteed. Further, each row of \mathbf{S} is a sample of randomly combined values between 0 and 1 that are mapped to its target distribution according to

$$\hat{x}_{ij} = F_{x_j}^{-1}(s_{ij}) \quad (3)$$

where $F_{x_j}^{-1}$ is the inverse of the cumulative probability function of variable x_j . The outputs \hat{x}_{ij} forms a sample vector $\hat{\mathbf{x}}_i$ with parameters for one deterministic vehicle dynamics simulation.

6.4. *Robustness*

In order to find robust designs that are well adapted to the spread in traffic parameters, such as wheel profiles and vehicle types, some of this spread has been accounted for in the analyses by using samples of parameter settings in the evaluation of objective functions. In this thesis, the term robust should therefore be understood in the sense that some of the spread in traffic parameters is accounted for, which should result in optimised designs that are better suited for the traffic situation in track than if the optimisation was performed using only a single parameter setting. It could still be that different areas of turnout design have different sensitivity to the spread and change in traffic parameters in themselves. If for example the crossing is considered, it is anticipated that a reduction of rail pad stiffness will reduce the impact forces on the crossing (**Paper C**), and that a stronger material will reduce the degradation rate, regardless of the shapes of the passing wheel profiles. The performance of a given crossing geometry is however also dependent on how well it is adapted to the shapes of the passing wheel profiles. In this sense the area of geometry optimisation is less robust than the previously mentioned design areas, but not less important as the large wheel–rail contact forces in turnouts are much due to the discontinuous rail profiles as described in Sections 2 and 3.

The representativeness of a sample that accounts for some of the spread in traffic parameters is of course highly dependent on whether the most influential parameters are considered in the sample. The parameter selections for the studies of this thesis are mainly based on a study covering the stochastic spread of traffic parameters in switches [43]. An example of a more explicit application of robust design methodology in a railway setting can be found in [44].

6.5. *Comments on methodology*

It is not necessarily the case that an optimised rail design fresh from the computer leads to lower LCC when implemented in track, as it, for example, might be more expensive to manufacture or simply the wrong design because the simulation model is not good enough. It is however hard to imagine a problem formulation for an optimisation where all LCC-affecting parameters of the turnout are known and considered at once. Therefore the activities in the present project can in a sense be regarded as being part of a multidisciplinary turnout optimisation where researchers, turnout manufacturers and infrastructure managers all seek improvements within their area of expertise. Suggested improvements can then be fed into the railway community for evaluation against the global objective of minimised LCC and compliance to regulations and other requirements.

It is proposed that a railway system can be described as a system with high causal density in the meaning that many parameters interact and affect the dynamic vehicle–track interaction and track degradation. The high causal density makes it difficult to predict what the consequences will be from a single parameter change and how it will impact the LCC. In addition to simulation based investigations, field evaluations of novel technologies are therefore of utmost importance. In such experiments, it is important that the stochastic

spread in performance between individual copies of components is quantified and accounted for.

In the field evaluation of the influence of rail pad stiffness on vertical impact force during crossing transition presented in **Paper C**, it is most likely sufficient to evaluate only one turnout (and an unaltered reference) to find the relation between these two quantities. To fully evaluate the effect on LCC however, a wider assessment is most likely necessary. For example, a softer rail pad will induce increased rail bending that may increase the risk of fatigue failures. To address such uncertainties, one method could be to apply the concept of randomised field trials from medical and social sciences [45] or other forms of experimental designs [46]. Then different design solutions or maintenance strategies could be applied to different groups of turnouts and their long term performance could be assessed. The number of turnouts in each group would have to be large enough to control the variance in the LCC estimate for each group. This is important as the variance will affect the possibilities to determine the significance of any difference in observed performance between different turnout groups. It is noted that such trials could imply significant costs. On the other hand the number of turnouts in each trial would still be small compared to the total number of turnouts in the network, and the results obtained conclusive with regards to LCC costs if the study is of good quality. If novel designs are introduced in the full network, based on the evaluation of individual turnouts, it can prove to be a costly mistake if the LCC performance of the novel design is worse than the old one.

7. Summary of Appended Papers

7.1. Paper A

A methodology for the simulation of degradation of rail profiles in switches & crossings (S&C) is presented. The methodology includes: simulation of dynamic vehicle-track interaction considering stochastic variations in input data (such as wheel profile, train speed and wheel-rail friction coefficient), simulation of wheel-rail contacts accounting for non-linear material properties and plasticity, and simulation of wear and plastic deformation in the rail during the life of the S&C component. The methodology is demonstrated by predicting the damage of a switch rail profile, manufactured from R260 steel, when subjected to freight traffic in the diverging route (facing move). In particular, the consequences of increasing the axle load from 25 tonnes to 30 tonnes are studied.

7.2. Paper B

Dynamic interaction between a railway freight vehicle and an S&C is studied by simulations of vehicle dynamics. In particular, the influence of a stochastic spread (scatter) in traffic parameters on damage in the S&C is assessed. The considered parameters are wheel profile and wheel-rail friction coefficient. To form a database for sampling, 120 wheel profiles from freight wagons in regular traffic have been measured and categorised with respect to wear. Among the investigated parameters, it is shown that equivalent conicity is the wheel profile parameter correlating best to damage in the S&C panels. The influence of hollow worn wheels on damage is also investigated, and it is found that such wheel profiles display a different running behaviour at the crossing transition. Convergence properties for samples of runs generated by Latin Hypercube Sampling (LHS) are compared with the corresponding properties obtained by pure random sampling. It is concluded that the LHS-generated samples exhibit similar or smaller variance in damage compared with the randomly generated samples.

7.3. Paper C

A model for simulation of dynamic interaction between a railway vehicle and a turnout is validated versus field measurements. In particular, the implementation and accuracy of viscously damped track models with different complexity are assessed. The validation data comes from full-scale field measurements of dynamic track stiffness and wheel-rail contact forces in a demonstrator turnout that was installed as part of the INNOTRACK project with funding from the European Union Sixth Framework Programme. Vertical track stiffness at nominal wheel loads, in the frequency range up to 20 Hz, was measured using a rolling stiffness measurement vehicle (RSMV). Vertical and lateral wheel-rail contact forces were measured by an instrumented wheelset mounted in a freight car featuring Y25 bogies. The measurements were performed for traffic both in the through and diverging routes, and in the facing and trailing moves. The full set of test runs was repeated with different types of rail pad to investigate the influence of rail pad stiffness on contact forces. It is concluded that impact forces on the crossing can be reduced by using more resilient rail pads. To allow for vehicle dynamics simulations at low computational cost, the track models are discretised space-variant mass-spring-damper models that are moving with each wheelset of the vehicle model. Acceptable agreement between simulated and measured vertical contact forces at the crossing can be obtained when the standard GENSYS track model is extended with one ballast/subgrade mass per rail side. This model

can be tuned to capture the large phase delay in dynamic track stiffness at low frequencies, as measured by the RSMV, while remaining sufficiently resilient at higher frequencies.

7.4. Paper D

A methodology for the optimisation of a prescribed track gauge variation (gauge widening) in the switch panel of a railway turnout (switch and crossing, S&C) is presented. The aim is to reduce rail profile degradation. A holistic approach is applied, where both routes and travel directions (moves) of traffic in the switch panel are considered simultaneously. This is made possible by a parameterisation that links the switch rail geometry to the parameterised gauge. As cross-sections are moved longitudinally to alter the thickness of the switch rails, also the switch rail height is a dependent variable. The problem is formulated as a multi-objective minimisation problem which is solved using a genetic-type optimisation algorithm which provides a set of Pareto optimal solutions. The dynamic vehicle–turnout interaction is evaluated using a multibody simulation tool and the energy dissipation in the wheel–rail contacts is used for the assessment of gauge parameters. Two different vehicle models are used, one freight car and one passenger train set, and a stochastic spread in wheel profile and wheel–rail friction coefficient is accounted for. It is found that gauge configurations with a large gauge-widening amplitude for the straight stock rail are optimal for both the through and diverging routes, while the results for the curved stock rail show a larger route dependence. The optimal gauge configurations are observed to be similar for both vehicle types.

7.5. Paper E

Inspired by a manufacturing process of switch rails for railway turnouts, a method for the optimisation of switch rail profile geometry is presented. The switch rail profile geometry is parameterised with four design variables to define a B-spline curve for the milling tool profile, and two design variables to prescribe the deviation from the nominal vertical path of the milling tool. The optimisation problem is formulated as a multi-objective minimisation problem with objective functions based on the contact pressure and the energy dissipation in the wheel–rail contact. The front of Pareto optimal solutions is determined by applying a genetic type optimisation algorithm. The switch rail profile designs are evaluated by simulations of dynamic vehicle–turnout interaction. It is concluded that the obtained set of Pareto optimal solutions corresponds to a rather small variation in design variables where increased profile height and increased profile shoulder protuberance are preferred for both objectives. The improvement in the objectives comes at the cost of an earlier wheel transition to the switch rail and thus increased vertical loading at a thinner rail cross-section. The performance of the optimised geometry is evaluated using a set of 120 measured wheel profiles, and it is shown that the optimised geometry reduces damage also for this large load collective. It is concluded that accurate limits on switch rail loading need to be established to determine the feasible design space for switch rail geometry optimisation.

7.6. Paper F

A numerical method for robust geometry optimisation of railway crossings is presented. The robustness is achieved by optimising the crossing geometry for a representative set of wheel profiles. As a basis for the optimisation, a crossing geometry is created where rail cross-section profiles and longitudinal height profiles of both wing rails and crossing nose

are parameterised. Based on the approximation that the two problems are decoupled, separate optimisations are performed for the cross-sectional rail profiles and the longitudinal height profiles. The rail cross-sections are optimised to minimise the maximum equivalent Hertzian wheel–rail contact pressure. The longitudinal height profiles are optimised to minimise the accumulated damage in the wing rail to crossing nose transition zone. The accumulated damage is approximated using an objective criterion that accounts for the angle of the wheel trajectory reversal when each wheel profile makes the transition from the wing rail to the crossing nose as well as the distribution of transition points for the utilised wheel profile set. It is found that small non-linear height deviations from a linear longitudinal wing rail profile in the transition zone can reduce the objective compared to the nominal design. Also the relation between spread in wheel profile geometry, transition zone length and dip magnitude of the vertical wheel trajectories is investigated. It is demonstrated that the variation in wheel profiles shapes, lateral wheel displacements and the feasible transition zone length will determine the inclinations of the wing rail and crossing nose if all wheel profiles are to make their transition in the transition zone.

8. Contributions of the Thesis

Based on a comparison of the literature review in Section 5 and the contents of this thesis, the author would like to highlight the following contributions to the field of railway turnout optimisation. Any excessive claims are the sole responsibility of the present author.

- The illustration of the kinematic and dynamic consequences associated with turnout rail geometry by comparing simulation cases with turnout and standard rails in Section 3.
- The studies in **Paper B** on the correlation between wheel profile characterisation parameters and damage in S&C allow for more efficient sampling using Latin Hypercube Sampling in the generation of representative traffic load samples.
- The use of a multi-objective optimisation approach to highlight the design trade-off in performance between different traffic routes for gauge optimisation in **Paper D**. This investigation is conducted using a parameterisation that links the switch rail geometry to the gauge widening.
- An illustration of the different optima found depending on whether a sample of wheel profiles or a single nominal wheel profile is accounted for in the through route gauge optimisation of **Paper D**.
- The development of drawing-inspired and spline-based parameterised geometries of switch rails and crossings with a high level of design freedom for **Papers E** and **F**.
- Rail profile optimisation is a common topic in railway mechanics, but little information has been found about rail profile optimisation in the switch panel as presented in **Paper E**.
- An investigation and demonstration of the constraints imposed on crossing geometry design by the spread in shape and lateral displacement of passing wheels in **Paper F**. A part of this investigation was also the strong correlation found between wheel profile shape and position of the point of transition between wing rail and crossing nose.
- Creation of a meta-model approach in **Paper F** for the optimisation of the longitudinal height profiles in a crossing geometry. The meta-model is computationally efficient and makes it possible to account for very large samples of measured wheel profiles. The optimisation routine could also be used to design the crossing geometry for a given distribution of the transitions from wing rail to crossing nose.
- Quantification of the transition point distributions due to a spread in wheel profile shapes for the stock rail to switch rail transition in the switch panel (**Paper E**) and wing rail to crossing nose transition in the crossing (**Paper F**).

9. Concluding Remarks and Future Work

In this thesis, methods for robust geometry optimisation of S&C have been presented. To a large extent this work can be considered to be rooted in, and have become an extension of, the turnout optimisation studies previously performed in INNTRACK [25, 27].

9.1. Methodological comments

In the view of the author, the main limitation of the presented optimisation methods is that they only in a qualitative sense account for the load limits (strength) of the rails. For example the constraint on the minimum nominal switch rail thickness that can be assumed to carry the full wheel load in **Paper E**, or a limit on the available transition zone in the crossing in **Paper F**.

On the other hand, the methods already account for a load collective that can be expanded if necessary. This means that if a model is developed that can estimate for example the accumulated fatigue damage, it opens up for the possibility to perform optimisations that make better use of the information in a load collective. The criteria for accumulated damage would thus need to be much more computationally efficient than those presented in for example **Paper A** and [18].

The optimisation papers (**Papers D, E and F**) in the thesis are mainly focused on methods and results. For future work it could be of interest to perform parameter sensitivity studies to obtain more qualitative information about the problems at hand.

As rail inclination will affect the conicity properties of the wheel–rail interaction and thus also the sensitivity of the passing wheelsets to the asymmetric rail profile configuration in the switch panel, it would be interesting to re-run the optimisations of **Paper D** for switch panels constructed from rails with different levels of inclination and/or states of wear.

At the IAVSD (International Association for Vehicle System Dynamics) symposium in Qingdao, China, in the summer of 2013, Prof. Shabana challenged the railway community to move from the “miniprof”-paradigm of describing rail profiles as rail cross-sections to the “CAD”-paradigm where the rails are described as a 3D-surface. This idea is interesting for the wheel–rail contact in switches and crossings which typically relies on interpolated geometry or contact point functions between discrete cross-sections. It is the view of the present author that this challenge should be taken seriously.

9.2. Implementation

The idea of accounting for load collectives in the optimisation of S&C opens up for customised design and maintenance of turnouts for given traffic situations, or at least different categories of traffic situations. For example, switches could be optimised for the traffic distribution between routes and moves using the methods of **Paper D** or the transition points in the crossing could be distributed according to the dominating traffic direction using the methods of **Paper F**.

Design and maintenance customisation also requires more knowledge of the traffic situation as well as status and history of individual turnouts. Considering the capabilities of information technology, the technical prerequisites for such considerations are already present [47].

For the present author, especially the studies of **Paper F** highlight how interconnected a railway system is. As demonstrated in the paper, the wing rail and crossing nose inclinations are directly connected to the length of the feasible transition zone, the spread

of wheel profile shapes in traffic and the check rail tolerances that to a large extent determine the range of lateral wheel positions as the wheels negotiates a crossing.

As the longitudinal inclination of the wing rail and crossing nose will determine the vertical wheel trajectory of the passing wheels and thus also the impact angle and the corresponding impact force during the transition from wing rail to crossing nose and vice versa, the possible design improvements and damage reductions for crossings are to a large extent dependent on the maintenance tolerances of wheel profiles and check rails. In order to find a better basis for decisions on maintenance, the cost of wheel re-profiling needs to be weighed against the potential reduction in crossing (and other) damage. If the geometric spread of wheels in traffic is smaller, and the impact damage in crossings could be reduced due to less interference contact and/or reduced impact angles through smaller inclinations of the wing rail and crossing nose, money would be saved in that end.

Simulations of mechanical systems typically represent a bottom-up approach where design improvements are sought through studies of the mechanical performance for the system at hand. The complementary approach is the bottom-down approach where key performance indicators for components in track, such as maintenance costs, are studied for different designs to see what design solutions actually work better in practice. In the (not very unique) view of the present author, simulations and design studies are useful tools to come up with good design solutions, but more or less certain knowledge about the practical value of different designs can only be obtained from studies of actual performance in track. This is because the railway system can be characterised as a system of high causal density where many parameters interact to form the actual performance and it is difficult, sometimes maybe impossible, to foresee all the consequences of a single parameter change. Therefore it is also proposed that designed experiments should be considered for the evaluation of design changes in the railway system as discussed in Section 6.5.

10. References

- [1] E. Andersson, M. Berg, and S. Stichel, *Rail vehicle dynamics*, Department of Aeronautical & Vehicle Engineering, KTH (The Royal Institute of Technology), Stockholm, 2007.
- [2] S. Iwnicki (ed.) *Handbook of railway vehicle dynamics*, CRC Taylor & Francis, Boca Raton, FL, 2006.
- [3] C. Esveld, *Modern railway track*, 2nd ed., Delft MRT-Productions, 2001.
- [4] E. Kassa, *Dynamic train-turnout interaction: mathematical modelling, numerical simulation and field testing*, PhD Thesis, Department of Applied Mechanics, Chalmers University of Technology, Göteborg, 2007.
- [5] CEN, *EN 13232-1, Railway applications – Track – Switches and crossings – Part 1: Definitions*, 2003.
- [6] T. Dahlberg, M. Ekh, J.C.O. Nielsen, and J.H. Sällström, *State-of-the-art study on railway turnouts: dynamics and damage*, Research Report 2004:8, Department of Applied Mechanics, Chalmers University of Technology, Göteborg, 2004.
- [7] A. Nissen, *Development of life cycle cost model and analyses for railway switches and crossings*, Ph.D. Thesis, Department of Civil, Mining and Environmental Engineering, Luleå University of Technology, Luleå, 2009.
- [8] A. Nissen, *Analys av statistik om spårväxlar underhållsbehov (analysis of statistics of maintenance requirements for railway turnouts, in Swedish)*, Licentiate Thesis, JvtC - Järnvägstekniskt Centrum (Railway Engineering Centre), Luleå University of Technology Luleå, 2005.
- [9] A. Ekberg, and B. Paulsson (eds.), *INNOTRACK: Concluding technical report*, International Union of Railways (UIC), Paris, 2010, 288 pp.
- [10] W. Grönlund, and G. Baumann (eds.), *INNOTRACK: D3.1.1/D3.1.2 Definition of key parameters and Report on cost-drivers for goal-directed innovation*, www.innotrack.net, 2008, 37 pp.
- [11] GENSYS. DEsolver AB, Optand 914, S-831 92 Östersund; software available at: www.gensys.se
- [12] E. Kassa, and J.C.O. Nielsen, *Dynamic interaction between train and railway turnout: full-scale field test and validation of simulation models*, Vehicle System Dynamics 46 (S1) (2008), pp. 521-534.
- [13] J.R. Evans, and M.C. Burstow, *Vehicle/track interaction and rolling contact fatigue in rails in the UK*, Vehicle System Dynamics 44 (S1) (2006), pp. 708-717.
- [14] T.G. Pearce, and N.D. Sherratt, *Prediction of Wheel Profile Wear*, Wear 144 (1-2) (1991), pp. 343-351.
- [15] R. Lewis, and U. Olofsson (eds.), *Wheel-rail interface handbook*, CRC Press and Woodhead Publishing, Boca Raton, FL and Oxford, 2009.
- [16] C. Casanueva, P.-A. Jönsson, and S. Stichel, *Influence of switches and crossings on wheel profile evolution in freight vehicles*, Proceedings of the 23rd International Symposium on Dynamics of Vehicles on Roads and Tracks (IAVSD), Qingdao, China, 2013.
- [17] V.L. Markine, and I.Y. Shevtsov, *An experimental study on crossing nose damage of railway turnouts in the Netherlands*, Proceedings of the 14th International Conference on Civil, Structural and Environmental Engineering Computing, Cagliari, Sardinia, Italy, 2013.

- [18] D. Nicklisch, J.C.O. Nielsen, M. Ekh, A. Johansson, B. Pålsson, A. Zoll, and J. Reinecke, *Simulation of wheel–rail contact and subsequent material degradation in switches & crossings*, Proceedings of the 21st International Symposium on Dynamics of Vehicles on Roads and Tracks (IAVSD), Stockholm, Sweden, 2009.
- [19] A. Ekberg, E. Kabo, and H. Andersson, *An engineering model for prediction of rolling contact fatigue of railway wheels*, *Fatigue & Fracture of Engineering Materials & Structures* 25 (10) (2002), pp. 899-909.
- [20] voestalpine VAE GmbH, Alpinestrasse 1, 8740 Zeltweg, Austria, www.voestalpine.com/vae/.
- [21] J.R. Oswald, and G. Bishop, *Optimization of turnout layout- and contact-geometry through dynamic simulation of vehicle–track interaction*, Proceedings of the 7th International Heavy Haul Conference, Brisbane, Australia, 2001.
- [22] R.F. Lagos, A. Alonso, J. Vinolas, and X. Perez, *Rail vehicle passing through a turnout: analysis of different turnout designs and wheel profiles*, Proceedings of the Institution of Mechanical Engineers Part F-Journal of Rail and Rapid Transit 226 (F6) (2012), pp. 587-602.
- [23] M.R. Bugarin, and J.M.G. Diaz-de-Villegas, *Improvements in railway switches*, Proceedings of the Institution of Mechanical Engineers Part F-Journal of Rail and Rapid Transit 216 (4) (2002), pp. 275-286.
- [24] E. Kassa, S. Iwnicki, J. Perez, P. Allen, and Y. Bezin, *Optimization of track gauge and track stiffness along a switch using a multibody simulation tool*, Proceedings of 21st International Symposium on Dynamics of Vehicles on Roads and Tracks, Stockholm, Sweden, 2009.
- [25] J.C.O. Nielsen (ed.), *INNOTRACK: D3.1.5 Recommendation of, and scientific basis for, optimisation of switches & crossings – part 1*, www.innotrack.net, 2009, 30 pp.
- [26] D. Nicklisch, E. Kassa, J.C.O. Nielsen, M. Ekh, and S. Iwnicki, *Geometry and stiffness optimization for switches and crossings, and simulation of material degradation*, Proceedings of the Institution of Mechanical Engineers Part F-Journal of Rail and Rapid Transit 224 (F4) (2010), pp. 279-292.
- [27] J.C.O. Nielsen (ed.) *INNOTRACK: D3.1.4 Summary of results from simulations and optimisation of switches*, www.innotrack.net, 2008, 38 pp.
- [28] V.L. Markine, M.J.M.M. Steenbergen, and I.Y. Shevtsov, *Combatting RCF on switch points by tuning elastic track properties*, *Wear* 271 (1-2) (2011), pp. 158-167.
- [29] H.H. Jenkins, J.E. Stephenson, G.A. Clayton, G.W. Morland, and D. Lyon, *The effect of track and vehicle parameters on wheel/rail vertical dynamic forces*, *Railway Engineering Journal* (January) (1974).
- [30] C. Wan, V.L. Markine, I.Y. Shevtsov, and R.P.B.J. Dollevoet, *Improvement of train–track interaction in turnouts by optimising the shape of crossing nose*, Proceedings of the 23rd International Symposium on Dynamics of Vehicles on Roads and Tracks (IAVSD), Qingdao, China, 2013.
- [31] C. Wan, and V.L. Markine, *A parametric study of the rail geometry at railway crossings*, Proceedings of 14th International Conference on Civil, Structural and Environmental Engineering Computing, Cagliari, Italy, 2013.
- [32] Z.S. Ren, S.G. Sun, and G. Xie, *A method to determine the two-point contact zone and transfer of wheel-rail forces in a turnout*, *Vehicle System Dynamics* 48 (10) (2010), pp. 1115-1133.

- [33] A.A. Shabana, *Dynamics of multibody systems*, 3rd ed., Cambridge University Press, Cambridge, U.K. ; New York, 2005.
- [34] A.A. Shabana, K.E. Zaaza, and H. Sugiyama, *Railroad vehicle dynamics a computational approach*, CRC Press, Boca Raton, FL, 2008.
- [35] T. Jendel, *Dynamic analysis of a freight wagon with modified Y25 bogies*, MSc Thesis, Department of Vehicle Engineering, KTH (The Royal Institute of Technology), Stockholm, 1997.
- [36] K.L. Johnson, *Contact mechanics*, Cambridge Univ. Press, Cambridge, 1985.
- [37] J.J. Kalker, *A fast algorithm for the simplified theory of rolling-contact*, *Vehicle System Dynamics* 11 (1) (1982), pp. 1-13.
- [38] *MATLAB*, The MathWorks, Inc., Natick, Massachusetts, United States.
- [39] K. Deb, *Multi-objective optimization using evolutionary algorithms*, *Wiley-Interscience series in systems and optimization*, Wiley, Chichester, 2001.
- [40] K. Deb, A. Pratap, S. Agarwal, and T. Meyarivan, *A fast and elitist multiobjective genetic algorithm: NSGA-II*, *IEEE Transactions on Evolutionary Computation* 6 (2) (2002), pp. 182-197.
- [41] M. Wahde, *Biologically inspired optimization methods: an introduction*, WIT Press, Southampton, 2008.
- [42] A. Olsson, G. Sandberg, and O. Dahlblom, *On Latin hypercube sampling for structural reliability analysis*, *Structural Safety* 25 (1) (2003), pp. 47-68.
- [43] E. Kassa, and J.C.O. Nielsen, *Stochastic analysis of dynamic interaction between train and railway turnout*, *Vehicle System Dynamics* 46 (5) (2008), pp. 429-449.
- [44] V.L. Markine, and I.Y. Shevtsov, *Optimization of a wheel profile accounting for design robustness*, *Proceedings of the Institution of Mechanical Engineers Part F- Journal of Rail and Rapid Transit* 225 (F5) (2011), pp. 433-441.
- [45] J. Manzi, *Uncontrolled*, Basic Books, New York, 2012.
- [46] G.E.P. Box, J.S. Hunter, and W.G. Hunter, *Statistics for experimenters: design, innovation and discovery*, 2nd ed., *Wiley series in probability and statistics*, Wiley-Interscience, Hoboken, N.J., 2005.
- [47] C.S. Bonaventura, A.M. Zarembski, and J.W. Palese, *Switch and crossing inspection and maintenace management using handheld computers*, *Proceedings of the 4th IET International Conference on Railway Condition Monitoring*, Derby, 2008.